The intersection of heavy ions and nuclear structure

from the neutron skin of ^{208}Pb to the unexpected uses of a nuclear bowling pin

Govert Nijs

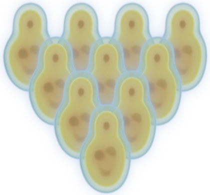

October 1, 2024

Based on:

- GN, van der Schee, 2312.04623
- Giacalone, GN, van der Schee, 2305.00015
- Giacalone, Bally, GN, Shen, Duguet, Ebran, Elhatisari, Frosini, Lähde, Lee, Lu, Ma, Meißner, Noronha-Hostler, Plumberg, Rodríguez, Roth, van der Schee, Somà, 2402.05995

The status of the field

- The general picture of the stages of a heavy ion collision is known.
- Theoretical modelling follows these stages:
  - TRENTo or IP-Glasma for the initial state.
  - Free streaming for the pre-hydrodynamic stage.
  - Viscous hydrodynamics with temperature dependent shear and bulk viscosity.
  - SMASH or UrQMD as a hadronic afterburner.
- Bayesian analysis gives a data-driven approach to understand each stage in more detail.

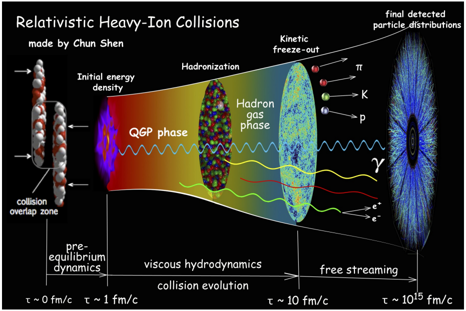

Uses of Bayesian analysis: viscosities

- We know the QGP phase is described by viscous hydrodynamics.
  - We know exactly what the free parameters are, i.e. η/s, ζ/s, ...
- We can use Bayesian analysis to find data-preferred values for these parameters.
- The values of the parameters provide an interface with microscopic theories of the QGP.

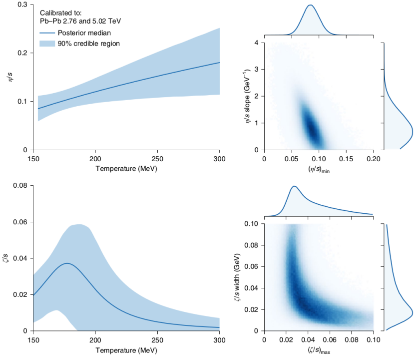

Uses of Bayesian analysis: parameterized phenomenology

$$\mathcal{T} \propto \left(\frac{\mathcal{T}_A^p + \mathcal{T}_B^p}{2} \right)^{1/p}$$

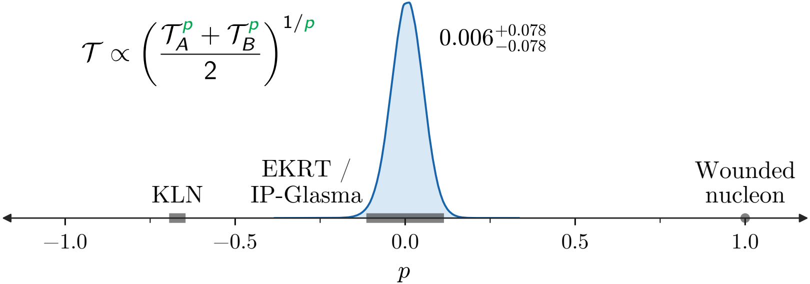

- For the initial state, there is no single widely accepted model.
- With a phenomenological model such as TRENTo, aspects of microscopic models can be tested, such as the scaling shown here, parameterized by p.
  - IP-Glasma and EKRT are ruled in.
  - KLN and wounded nucleon are ruled out.

Uses of Bayesian analysis: deciding between models

- One can take this idea a step further, and actually compare different models.
- Here shown are different particlization schemes.
- By taking into account how well each model fits, one can even take a weighted average over models, known as *Bayesian model averaging*.

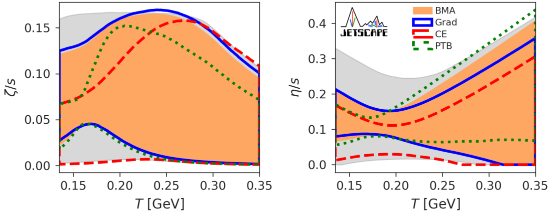

[JETSCAPE, 2010.03928]

Model used: *Trajectum*

- New heavy ion code developed in Utrecht/MIT/CERN.
  - *Trajectum* is the old Roman name for Utrecht.
- Contains initial stage, hydrodynamics and freeze-out, as well as an analysis suite.
- Easy to use, example parameter files distributed alongside the source code.
- Fast, fully parallelized.
  - Figure (20k oversampled PbPb events at 2.76 TeV) computes on a laptop in 21h.
  - Bayesian analysis requires $\mathcal{O}(1000)$ similar calculations to this one.
- Publicly available at sites.google.com/view/govertnijs/trajectum/.

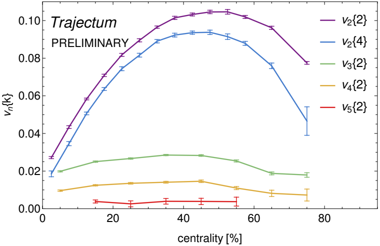

Some simple intuition

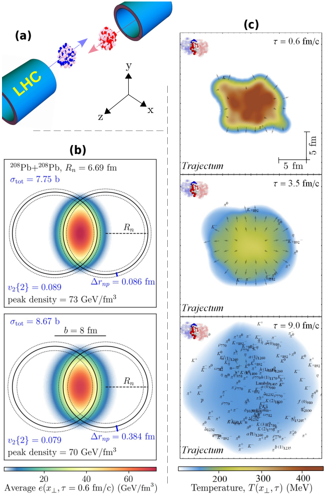

- Model details are not necessary to understand the contents of this talk.
  - Some details are available in the backup.
- Hydrodynamics can be intuitively understood:
  - Pressure gradients drive expansion.
  - Hotter systems expand faster, resulting in more transverse momentum.
  - Spatially anisotropic systems expand preferentially along the short axis, resulting in momentum anisotropy in the final state.

[Ollitrault, *Phys. Rev. D* **46** (1992), 229; Giacalone, GN, van der Schee, 2305.00015]

Bayesian analysis workflow

- In principle, Bayesian analysis is simply a fit to data.
- In practice the process is more complicated:
  - Generate a large number of randomly chosen parameter sets called *design points*.
  - Run the model for each one to obtain the prior.
  - Train the emulator.
  - Run the MCMC to obtain the posterior.
- The posterior then is a list of likely parameter sets.

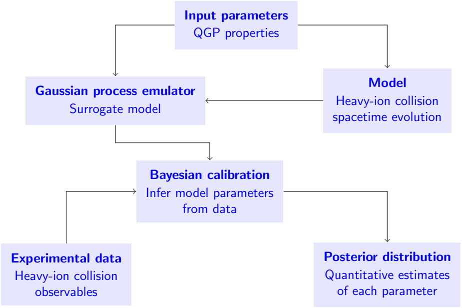

Bayesian analysis workflow

- In principle, Bayesian analysis is simply a fit to data.
- In practice the process is more complicated:
  - Generate a large number of randomly chosen parameter sets called *design points*.
  - Run the model for each one to obtain the prior.
  - Train the emulator.
  - Run the MCMC to obtain the posterior.
- The posterior then is a list of likely parameter sets.

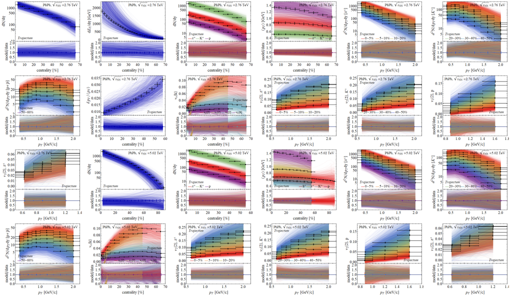

[GN, van der Schee, 2304.06191; Giacalone, GN, van der Schee, 2305.00015]

Bayesian analysis workflow

- In principle, Bayesian analysis is simply a fit to data.
- In practice the process is more complicated:
    - Generate a large number of randomly chosen parameter sets called *design points*.
    - Run the model for each one to obtain the prior.
    - Train the emulator.
    - Run the MCMC to obtain the posterior.
- The posterior then is a list of likely parameter sets.

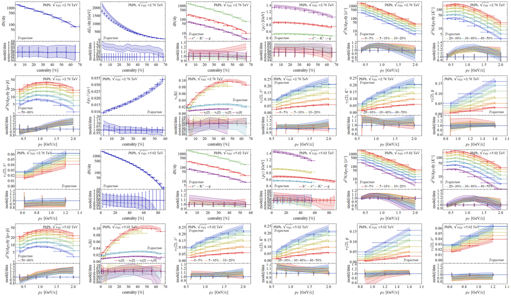

Bayesian analysis workflow

- In principle, Bayesian analysis is simply a fit to data.
- In practice the process is more complicated:
    - Generate a large number of randomly chosen parameter sets called *design points*.
    - Run the model for each one to obtain the prior.
    - Train the emulator.
    - Run the MCMC to obtain the posterior.
- The posterior then is a list of likely parameter sets.

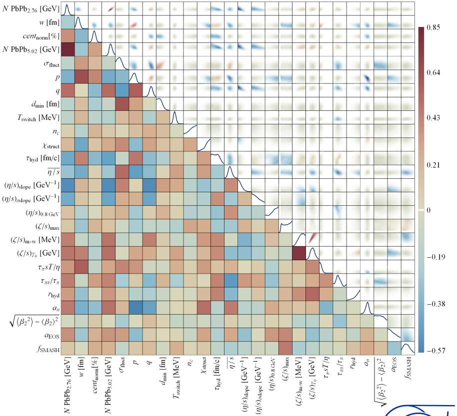

Data used: 670 individual data points

✓: data used
🕓: data available
✗: data unavailable

	PbPb 2.76 TeV				PbPb 5.02 TeV				pPb 5.02 TeV
	incl.	$\pi^\pm$	$K^\pm$	p	incl.	$\pi^\pm$	$K^\pm$	p	incl.
σ	✗	✗	✗	✗	✓	✗	✗	✗	✓
dN/dy	✓	✓	✓	✓	✓	✓	✓	✓	🕓
$\langle p_T \rangle$	✗	✓	✓	✓	✓	✓	✓	✓	🕓
$dE_T/d\eta$	✓	✗	✗	✗	✗	✗	✗	✗	✗
$\delta p_T/\langle p_T \rangle$	✓	✗	✗	✗	✗	✗	✗	✗	✗
$v_{2,3,4}\{2\}$	✓	🕓	🕓	🕓	✓	🕓	🕓	🕓	🕓
$v_2\{4\}$	✓	✗	✗	✗	✓	🕓	🕓	🕓	🕓
$d^2N/dp_T dy$	✗	✓	✓	✓	✗	✓	✓	✓	✗
$v_2\{2\}(p_T)$	✗	✓	✓	✓	✗	✓	✓	✓	🕓
$v_3\{2\}(p_T)$	✗	✓	🕓	🕓	✗	✓	🕓	🕓	🕓
$NSC(2,3)$	🕓	✗	✗	✗	✓	✗	✗	✗	🕓
$NSC(2,4)$	🕓	✗	✗	✗	✓	✗	✗	✗	🕓
$\rho(v_2\{2\}^2, \langle p_T \rangle)$	✗	✗	✗	✗	✓	✗	✗	✗	✗

[Giacalone, GN, van der Schee, 2305.00015]

Using the posterior parameter values to make predictions

- The posterior parameter values can be used to make predictions for new observables.
  - When using multiple samples from the posterior, this includes systematic uncertainty from the parameter estimation.
- Here shown is the prediction for ultracentral $\langle p_T \rangle$.

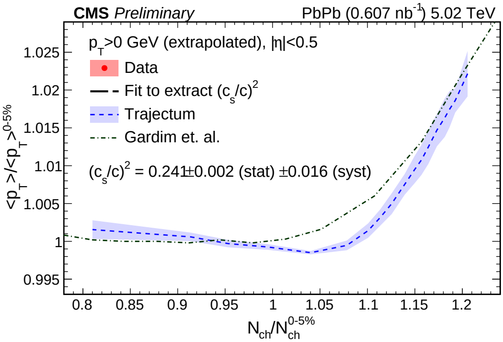

Using the posterior parameter values to make predictions

- The posterior parameter values can be used to make predictions for new observables.
  - When using multiple samples from the posterior, this includes systematic uncertainty from the parameter estimation.
- Here shown is the prediction for ultracentral $\langle p_T \rangle$.
- Precise agreement between theory and experiment.

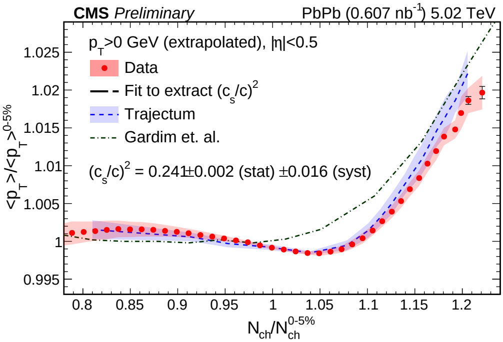

Neutron skin

- In a ^{208}Pb nucleus, neutrons sit further from the center than protons.
  - This is quantified by the *neutron skin*:

$$\Delta r_{np} = \langle r^2 \rangle_n^{1/2} - \langle r^2 \rangle_p^{1/2},$$

    i.e. the *difference* in RMS radii of the neutron and proton distributions.
- Heavy nuclei and neutron stars are sensitive to the same nuclear interactions.
  - A constraint on Δr_{np} translates directly into a constraint on the radius of a $1.4 M_\odot$ neutron star.
  - We can learn something about the low T, high μ_B region even at LHC energies!

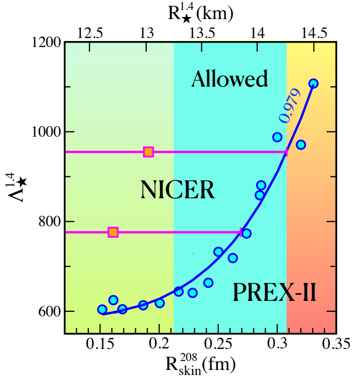

How to measure neutron skin?

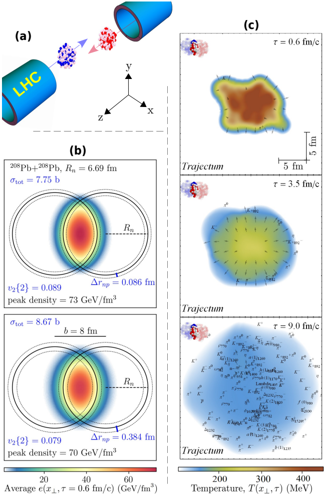

- To measure the neutron skin, we need the distributions of protons and neutrons inside the nucleus.
  - The proton distribution distribution is well-known from electron scattering.
- Several different methods are in use for the neutron distribution:
  - Polarized electron scattering off ^{208}Pb (PREX).
  - Photon tomography of ^{197}Au (STAR).
- Heavy ion collisions provide a completely orthogonal method.
  - Sensitive to the total matter distribution inside the nucleus.
  - Purely gluonic measurement.

The Woods-Saxon distribution

- Nucleon positions are drawn from a Woods-Saxon distribution:

$$\rho_{\text{WS}}(r) \propto \frac{1}{1 + \exp\left(\frac{r-R}{a}\right)}.$$

  - We fix R for both protons and neutrons.
  - We fix a for protons, while varying a_n as a parameter.

- Neutron skin $\Delta r_{np} = \langle r^2 \rangle_n^{1/2} - \langle r^2 \rangle_p^{1/2}$ strongly depends on a_n:

$$\langle r^2 \rangle_{\text{WS}} = \frac{12a^2 \, \text{Li}_5\left(-e^{R/a}\right)}{\text{Li}_3\left(-e^{R/a}\right)}.$$

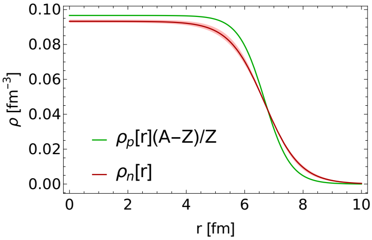

	proton	neutron
R [fm]	6.68	6.69
a [fm]	0.447	a_n

The Woods-Saxon distribution

- Nucleon positions are drawn from a Woods-Saxon distribution:

$$\rho_{\rm WS}(r) \propto \frac{1}{1+\exp\left(\frac{r-R}{a}\right)}.$$

  - We fix R for both protons and neutrons.
  - We fix a for protons, while varying a_n as a parameter.
- Neutron skin $\Delta r_{np} = \langle r^2 \rangle_n^{1/2} - \langle r^2 \rangle_p^{1/2}$ strongly depends on a_n:

$$\langle r^2 \rangle_{\rm WS} = \frac{12 a^2 \,{\rm Li}_5\left(-e^{R/a}\right)}{{\rm Li}_3\left(-e^{R/a}\right)}.$$

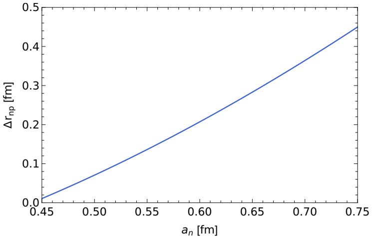

	proton	neutron
R [fm]	6.68	6.69
a [fm]	0.447	a_n

Do we have observables sensitive to a_n?

- Initial geometry is sensitive to a_n. Larger nuclei lead to:
  - Larger hadronic PbPb cross-section,
  - Larger initial QGP size,
  - Smaller initial QGP eccentricity.
- Final state observables are in turn sensitive to initial geometry. Larger Δr_{np} leads to:
  - Larger hadronic PbPb cross-section,
  - Smaller charged particle yield,
  - Smaller mean transverse momentum,
  - Smaller elliptic flow.

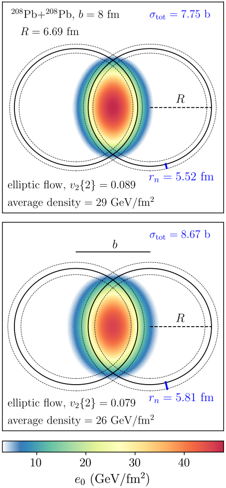

Do we have observables sensitive to a_n?

- Initial geometry is sensitive to a_n. Larger nuclei lead to:
  - Larger hadronic PbPb cross-section,
  - Larger initial QGP size,
  - Smaller initial QGP eccentricity.
- Final state observables are in turn sensitive to initial geometry. Larger Δr_{np} leads to:
  - Larger hadronic PbPb cross-section,
  - Smaller charged particle yield,
  - Smaller mean transverse momentum,
  - Smaller elliptic flow.

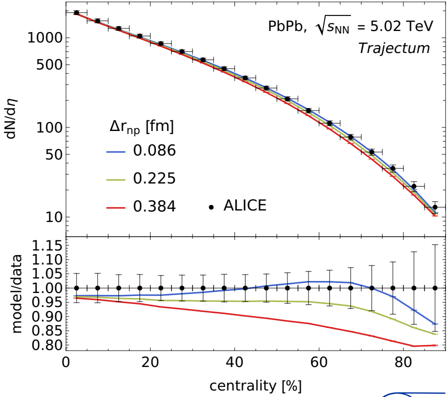

Do we have observables sensitive to a_n?

- Initial geometry is sensitive to a_n. Larger nuclei lead to:
  - Larger hadronic PbPb cross-section,
  - Larger initial QGP size,
  - Smaller initial QGP eccentricity.
- Final state observables are in turn sensitive to initial geometry. Larger Δr_{np} leads to:
  - Larger hadronic PbPb cross-section,
  - Smaller charged particle yield,
  - Smaller mean transverse momentum,
  - Smaller elliptic flow.

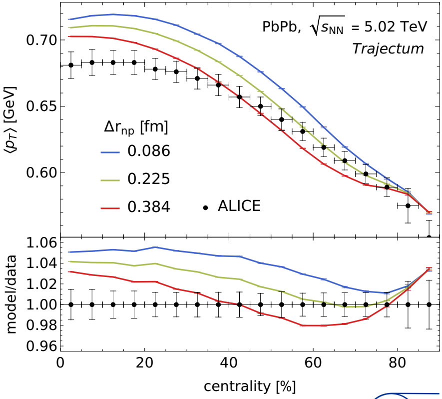

Do we have observables sensitive to a_n?

- Initial geometry is sensitive to a_n. Larger nuclei lead to:
  - Larger hadronic PbPb cross-section,
  - Larger initial QGP size,
  - Smaller initial QGP eccentricity.
- Final state observables are in turn sensitive to initial geometry. Larger Δr_{np} leads to:
  - Larger hadronic PbPb cross-section,
  - Smaller charged particle yield,
  - Smaller mean transverse momentum,
  - Smaller elliptic flow.

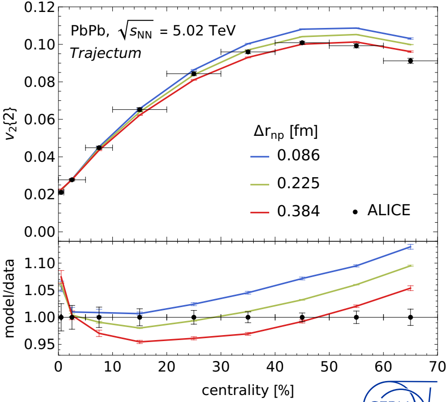

Bayesian analysis result using LHC data

- Resulting posterior for Δr_{np} is compatible with PREX II and ab initio nuclear theory.
- Slightly stronger constraint than PREX II ($\Delta r_{np} = 0.283 \pm 0.071$).
- Result is in principle improvable with better Bayesian analyses.
  - May be hard to do in practice.
  - The current analysis already took 2M CPUh.

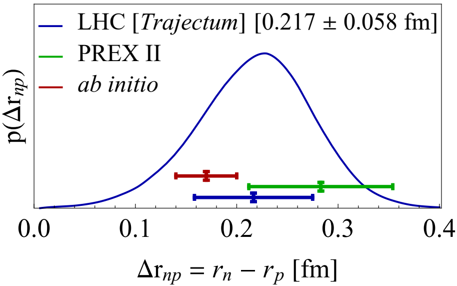

One fluid to rule them all?

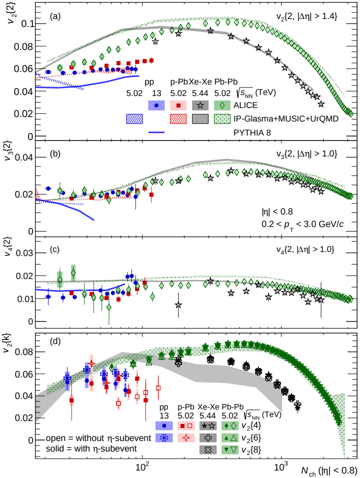

- Anisotropic flow is present in a great range of system sizes:
  - PbPb,
  - High multiplicity *p*Pb,
  - High multiplicity *pp*,
  - . . .
- Is this a sign of hydrodynamics?
  - Hydrodynamical simulations seem to work reasonably well.
  - But can a system that small really behave hydrodynamically?
  - Initial state geometry is poorly understood.
- We need a precision test of hydrodynamics in small systems.

Recap: why do we believe PbPb is hydrodynamic?

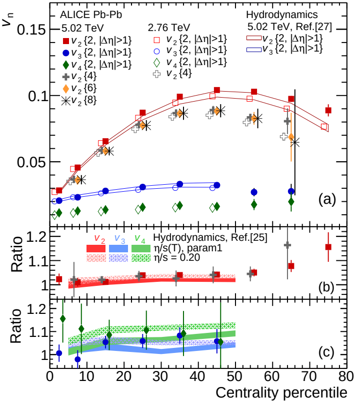

- Not just the presence of $v_n\{k\}$.
- We understand where the $v_n\{k\}$ come from!
  - Hydrodynamics converts initial state anisotropic geometry into final state momentum anisotropy.
  - We understand very well what the initial geometry looks like!
- For pPb this is not the case.
  - There is $v_n\{k\}$ measured.
  - But we do not understand the initial geometry.
  - No clear interpretation of experimental results.

[ALICE, 1602.01119]

Posing a precise question

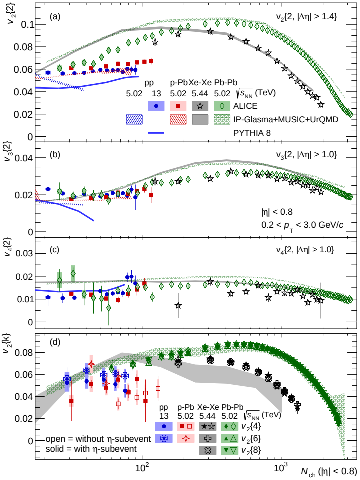

- Can we describe PbPb and a small system in a hydrodynamical model *with the same settings*?
  - Hydro model used should describe a wide range of PbPb observables.
- Can we find a quantity to predict which does not suffer from huge theoretical uncertainties? Wishlist:
  - Initial geometry under control.
  - Small sensitivity to proton substructure.
  - No longitudinal structure issues.
  - Quantifiable and small theory uncertainty.

[ALICE, 1903.01790]

Can $^{16}O^{16}O$ collisions help?

- $^{16}O^{16}O$ collisions are planned at the LHC for 2025.
- Shape of the proton and longitudinal structure are not an issue, but. . .

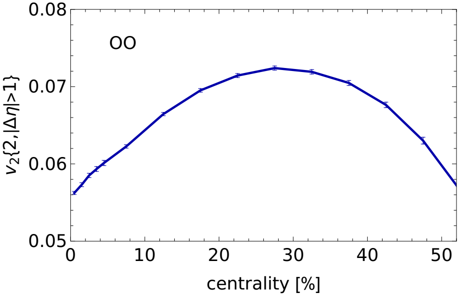

Can $^{16}O^{16}O$ collisions help?

- $^{16}O^{16}O$ collisions are planned at the LHC for 2025.
- Shape of the proton and longitudinal structure are not an issue, but. . .
- Magnitude of fluctuations in the initial state is poorly constrained.

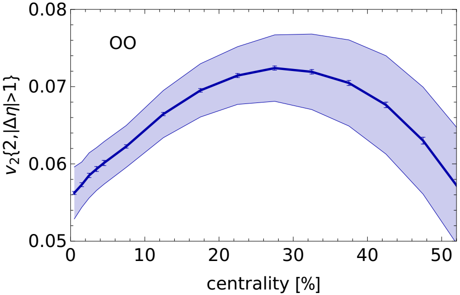

Can $^{16}O^{16}O$ collisions help?

- $^{16}O^{16}O$ collisions are planned at the LHC for 2025.
- Shape of the proton and longitudinal structure are not an issue, but...
- Magnitude of fluctuations in the initial state is poorly constrained.
- Different nuclear structure calculations give different answers!
- We have a handle on systematics, but errors are substantial.

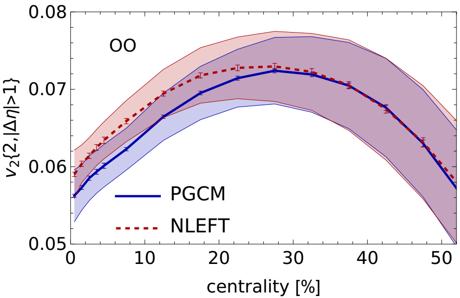

[Giacalone, Bally, GN, Shen et al., 2402.05995]

The nuclear bowling pin: ^{20}Ne

- We use both the PGCM and NLEFT frameworks for our nuclear structure input.
  - PGCM computes the average deformed densities.
  - NLEFT simulates an effective theory on a lattice.
- ^{16}O is shaped like an irregular tetrahedron.
- ^{20}Ne is close in size, but has the most extreme shape in the Segrè chart.
- Can we take a ratio between systems to cancel the uncertainties?

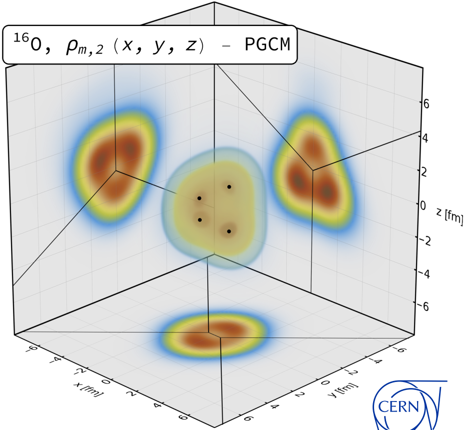

The nuclear bowling pin: ^{20}Ne

- We use both the PGCM and NLEFT frameworks for our nuclear structure input.
    - PGCM computes the average deformed densities.
    - NLEFT simulates an effective theory on a lattice.
- ^{16}O is shaped like an irregular tetrahedron.
- ^{20}Ne is close in size, but has the most extreme shape in the Segrè chart.
- Can we take a ratio between systems to cancel the uncertainties?

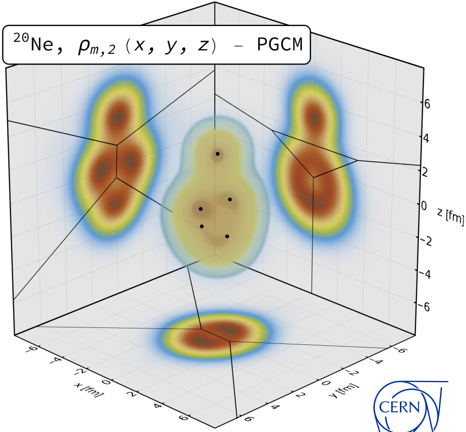

A careful look at uncertainties

- *Trajectum* systematic uncertainty contains contributions from:
  - Uncertainties in parameters.
  - Extrapolation to zero grid spacing.
- PGCM systematic uncertainty contains contributions from:
  - Sampling method: how to convert a density into a configuration.
  - Constraint application: order of operations in the PGCM computation.
- NLEFT systematic uncertainty contains contributions from:
  - Resolution of ambiguities from periodicity of the lattice.

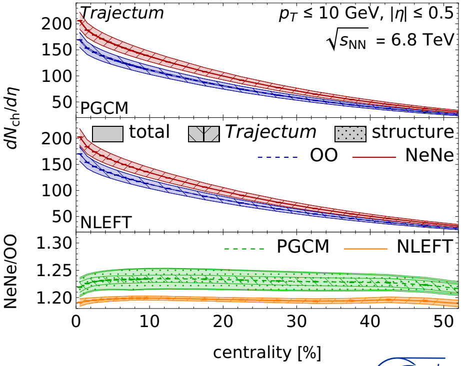

Comparing ^{20}Ne to ^{16}O significantly reduces errors!

- NLEFT and PGCM are consistent within uncertainties.
- Ratio of $v_2\{2\}$ reaches percent level precision from 5% to 20% centrality!
- Difference of $\rho(v_2\{2\}^2, \langle p_T \rangle)$ has uncertainty reduced by up to a factor 6!
- Larger PGCM uncertainty is mostly due to ambiguity in how to generate configurations from densities.

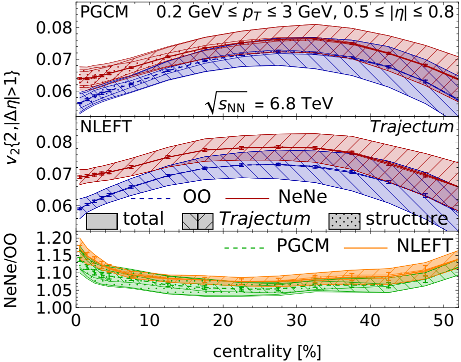

0–1%	$v_2\{2\}_{\text{NeNe}}/v_2\{2\}_{\text{OO}}$	$\rho_{2,\text{NeNe}} - \rho_{2,\text{OO}}$
NLEFT	$1.170(8)_{\text{stat.}}(30)^{\text{Traj.}}_{\text{syst.}}(0)^{\text{str.}}_{\text{syst.}}$	$-0.121(14)_{\text{stat.}}(10)^{\text{Traj.}}_{\text{syst.}}(0)^{\text{str.}}_{\text{syst.}}$
PGCM	$1.139(6)_{\text{stat.}}(27)^{\text{Traj.}}_{\text{syst.}}(28)^{\text{str.}}_{\text{syst.}}$	$-0.124(10)_{\text{stat.}}(10)^{\text{Traj.}}_{\text{syst.}}(29)^{\text{str.}}_{\text{syst.}}$

Comparing ^{20}Ne to ^{16}O significantly reduces errors!

- NLEFT and PGCM are consistent within uncertainties.
- Ratio of $v_2\{2\}$ reaches percent level precision from 5% to 20% centrality!
- Difference of $\rho(v_2\{2\}^2, \langle p_T \rangle)$ has uncertainty reduced by up to a factor 6!
- Larger PGCM uncertainty is mostly due to ambiguity in how to generate configurations from densities.

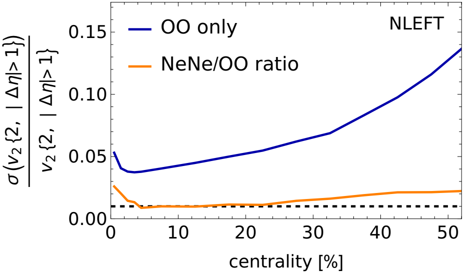

0–1%	$v_2\{2\}_{\mathrm{NeNe}}/v_2\{2\}_{\mathrm{OO}}$	$\rho_{2,\mathrm{NeNe}} - \rho_{2,\mathrm{OO}}$
NLEFT	$1.170(8)_{\mathrm{stat.}}(30)^{\mathrm{Traj.}}_{\mathrm{syst.}}(0)^{\mathrm{str.}}_{\mathrm{syst.}}$	$-0.121(14)_{\mathrm{stat.}}(10)^{\mathrm{Traj.}}_{\mathrm{syst.}}(0)^{\mathrm{str.}}_{\mathrm{syst.}}$
PGCM	$1.139(6)_{\mathrm{stat.}}(27)^{\mathrm{Traj.}}_{\mathrm{syst.}}(28)^{\mathrm{str.}}_{\mathrm{syst.}}$	$-0.124(10)_{\mathrm{stat.}}(10)^{\mathrm{Traj.}}_{\mathrm{syst.}}(29)^{\mathrm{str.}}_{\mathrm{syst.}}$

[Giacalone, Bally, GN, Shen et al., 2402.05995]

Comparing ^{20}Ne to ^{16}O significantly reduces errors!

- NLEFT and PGCM are consistent within uncertainties.
- Ratio of $v_2\{2\}$ reaches percent level precision from 5% to 20% centrality!
- Difference of $\rho(v_2\{2\}^2, \langle p_T \rangle)$ has uncertainty reduced by up to a factor 6!
- Larger PGCM uncertainty is mostly due to ambiguity in how to generate configurations from densities.

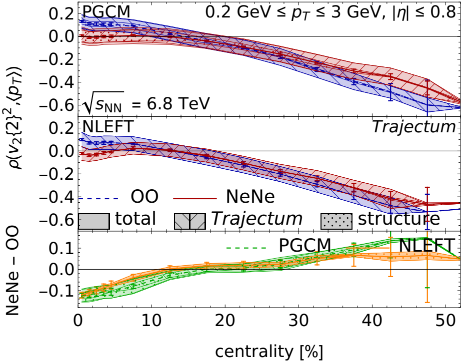

0–1%	$v_2\{2\}_{\mathrm{NeNe}}/v_2\{2\}_{\mathrm{OO}}$	$\rho_{2,\mathrm{NeNe}} - \rho_{2,\mathrm{OO}}$
NLEFT	$1.170(8)_{\mathrm{stat.}}(30)^{\mathrm{Traj.}}_{\mathrm{syst.}}(0)^{\mathrm{str.}}_{\mathrm{syst.}}$	$-0.121(14)_{\mathrm{stat.}}(10)^{\mathrm{Traj.}}_{\mathrm{syst.}}(0)^{\mathrm{str.}}_{\mathrm{syst.}}$
PGCM	$1.139(6)_{\mathrm{stat.}}(27)^{\mathrm{Traj.}}_{\mathrm{syst.}}(28)^{\mathrm{str.}}_{\mathrm{syst.}}$	$-0.124(10)_{\mathrm{stat.}}(10)^{\mathrm{Traj.}}_{\mathrm{syst.}}(29)^{\mathrm{str.}}_{\mathrm{syst.}}$

Comparing ^{20}Ne to ^{16}O significantly reduces errors!

- NLEFT and PGCM are consistent within uncertainties.
- Ratio of $v_2\{2\}$ reaches percent level precision from 5% to 20% centrality!
- Difference of $\rho(v_2\{2\}^2, \langle p_T \rangle)$ has uncertainty reduced by up to a factor 6!
- Larger PGCM uncertainty is mostly due to ambiguity in how to generate configurations from densities.

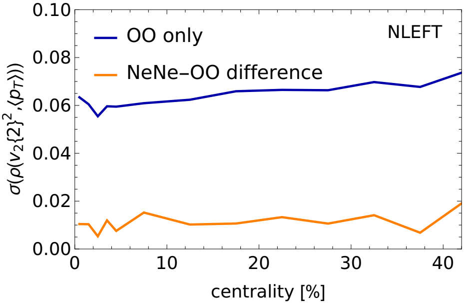

0–1%	$v_2\{2\}_{\text{NeNe}}/v_2\{2\}_{\text{OO}}$	$\rho_{2,\text{NeNe}} - \rho_{2,\text{OO}}$
NLEFT	$1.170(8)_{\text{stat.}}(30)^{\text{Traj.}}_{\text{syst.}}(0)^{\text{str.}}_{\text{syst.}}$	$-0.121(14)_{\text{stat.}}(10)^{\text{Traj.}}_{\text{syst.}}(0)^{\text{str.}}_{\text{syst.}}$
PGCM	$1.139(6)_{\text{stat.}}(27)^{\text{Traj.}}_{\text{syst.}}(28)^{\text{str.}}_{\text{syst.}}$	$-0.124(10)_{\text{stat.}}(10)^{\text{Traj.}}_{\text{syst.}}(29)^{\text{str.}}_{\text{syst.}}$

[Giacalone, Bally, GN, Shen et al., 2402.05995]

Conclusions

- Let us take another look at our wishlist:

$v_n\{k\}$ in	pPb	OO	NeNe/OO
Initial geometry under control	✗	✓	✓
Small sensitivity to proton substructure	✗	✓	✓
No longitudinal decorrelation issues	✗	✓	✓
Quantifiable theory uncertainty	✗	✓	✓
Small theory uncertainty	✗	$\geq 4\%$	$\geq 1\%$

- Theory has a much better handle on ^{16}O^{16}O compared to pPb.
- Theory uncertainties can be substantially reduced by supplementing ^{16}O^{16}O collisions with ^{20}Ne^{20}Ne collisions.
  - $v_2\{2\}$ ratio can be predicted to 1% precision between 5% and 20% centrality.
  - Different nuclear structure calculations give consistent results.

[Giacalone, Bally, GN, Shen et al., 2402.05995]

TH Institute: Light Ions at the LHC

Backup

Backup

Bayesian analysis details

- 3000 design points.
- 18k events per design point.
- Every 15th design point has 10× more statistics, enabling to emulate 'hard' observables such as $SC(n, m)$ and $\rho(v_2\{2\}^2, \langle p_T \rangle)$.

Error budget

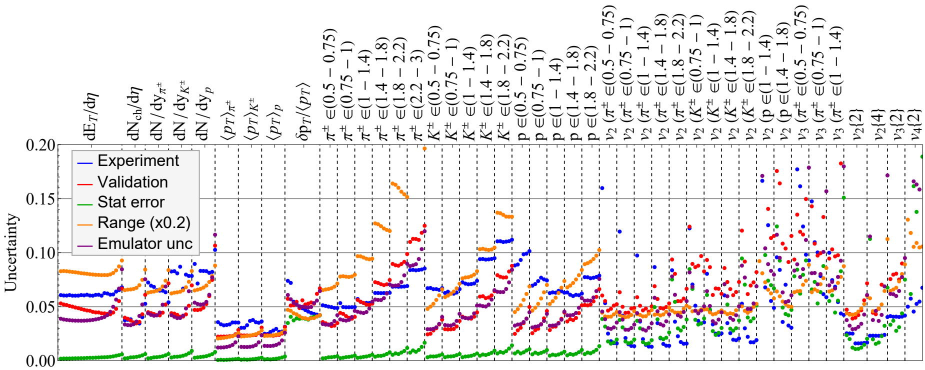

Posterior observables (1/3)

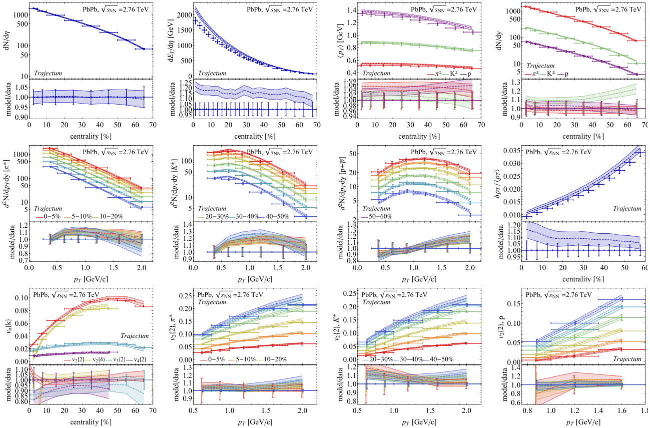

Posterior observables (2/3)

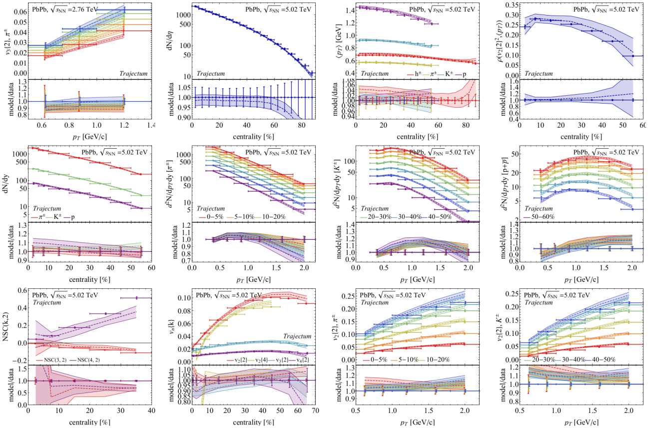

Posterior observables (3/3)

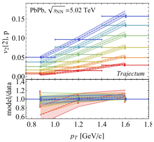

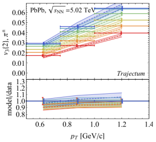

TRENTo initial conditions

- Nucleons A and B become *wounded* with probability

$$P_{\text{wounded}} = 1 - \exp\left(-\sigma_{gg} \int d\mathbf{x}\, \rho_A(\mathbf{x})\rho_B(\mathbf{x})\right), \quad \rho_A \propto \exp\left(\frac{-|\mathbf{x} - \mathbf{x}_A|^2}{2w^2}\right).$$

- Each wounded nucleon desposits energy into its nucleus's *thickness function* $\mathcal{T}_{A/B}$:

$$\mathcal{T}_{A/B} = \sum_{i \in \text{wounded A/B}} \gamma \exp(-|\mathbf{x} - \mathbf{x}_i|^2/2w^2),$$

with γ drawn from a gamma distribution with mean 1 and standard deviation σ_{fluct}.

- Actual formulas slightly modified because each nucleon has n_c constituents.

The TRENTo phenomenological ansatz

- The standard TRENTo formula combines thickness functions of the two nuclei $\mathcal{T}_A$ and $\mathcal{T}_B$ into a *reduced thickness* $\mathcal{T}$, interpreted as an energy density:

$$\mathcal{T} \propto \left(\frac{\mathcal{T}_A^p + \mathcal{T}_B^p}{2} \right)^{1/p},$$

with p a parameter.

- Some useful limits:

p	-1	0	1
$\mathcal{T}$	$\frac{2}{\frac{1}{\mathcal{T}_A}+\frac{1}{\mathcal{T}_B}}$	$\sqrt{\mathcal{T}_A \mathcal{T}_B}$	$\frac{\mathcal{T}_A+\mathcal{T}_B}{2}$

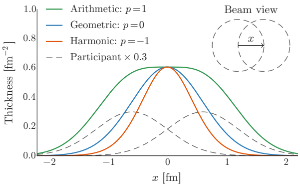

Free streaming pre-hydrodynamic stage

- TRENTo creates matter at proper time $\tau = 0^+$.
- Propagate the matter using free streaming:

$$T^{\mu\nu}(x, y, \tau_{\text{hyd}}) = \frac{1}{\tau_{\text{hyd}}} \int d\phi\, \hat{p}^\mu \hat{p}^\nu \mathcal{T}(x - \tau_{\text{hyd}} \cos\phi, y - \tau_{\text{hyd}} \sin\phi),$$

with

$$\hat{p}^\mu = \begin{pmatrix} 1 & \cos\phi & \sin\phi \end{pmatrix},$$

giving us the stress tensor $T^{\mu\nu}$ at proper time $\tau = \tau_{\text{hyd}}$.

- Here τ_{hyd} is the time at which hydrodynamics is started.
- The factor $1/\tau_{\text{hyd}}$ is due to longitudinal expansion.

Basics of hydrodynamics

- Hydrodynamics is the ultimate effective theory. Knowledge of the underlying microscopic theory is completely summarized in transport coefficients.
- Only conservation laws survive: equation of motion is simply

$$\partial_\mu T^{\mu\nu} = 0.$$

- Not enough equations to close the system. Need additional assumption of *local thermal equilibrium*.
- We write $T^{\mu\nu}$ in terms of building blocks T, u^μ, $g^{\mu\nu}$ and ∂_μ.

[Kovtun, 1205.5040; Glorioso, Liu, 1805.09331]

Hydrodynamics in the 14-moment approximation

- Define ($g^{\mu\nu} = \mathrm{diag}(1, -1, -1, -1)$):

$$\Delta^{\mu\nu} = g^{\mu\nu} - u^\mu u^\nu, \quad \nabla^\mu = \Delta^{\mu\nu}\partial_\nu, \quad D = u^\mu \nabla_\mu, \quad \sigma^{\mu\nu} = \nabla^{\langle\mu} u^{\nu\rangle},$$

  with $\langle\rangle$ symmetrizing and removing the trace.
- We solve viscous hydrodynamics without currents, i.e.

$$\partial_\mu T^{\mu\nu} = 0, \quad T^{\mu\nu} = e u^\mu u^\nu - (P + \Pi)\Delta^{\mu\nu} + \pi^{\mu\nu},$$

- $\pi^{\mu\nu}$ and Π follow the 14-moment approximation:

$$\begin{aligned} -\tau_\pi \Delta^\mu_\alpha \Delta^\nu_\beta D\pi^{\alpha\beta} &= \pi^{\mu\nu} - 2\eta\sigma^{\mu\nu} + \delta_{\pi\pi}\pi^{\mu\nu}\nabla\cdot u \\ &\quad - \phi_7 \pi^{\langle\mu}_\alpha \pi^{\nu\rangle\alpha} + \tau_{\pi\pi}\pi^{\langle\mu}_\alpha \sigma^{\nu\rangle\alpha} - \lambda_{\pi\Pi}\Pi\sigma^{\mu\nu}, \\ -\tau_\Pi D\Pi &= \Pi + \zeta\nabla\cdot u + \delta_{\Pi\Pi}\nabla\cdot u\Pi - \lambda_{\Pi\pi}\pi^{\mu\nu}\sigma_{\mu\nu}. \end{aligned}$$

[Denicol, Jeon, Gale, 1403.0962]

Particlization

- At the freeze-out temperature T_{sw}, we turn the fluid back into particles.
- Particles are sampled thermally, and boosted with the fluid velocity u^μ.
- We use the PTB prescription to match $\pi^{\mu\nu}$ and Π across the transition, so that $T^{\mu\nu}$ is smooth.
- After particlization, we use SMASH as a hadronic afterburner.

[Pratt, Torrieri, 1003.0413; Bernhard, 1804.06469; Weil et al., 1606.06642, Sjostrand, Mrenna, Skands, 0710.3820]

Fitting to the pPb and PbPb cross sections

- In the T$_R$ENTo model, the nucleon size is described by the Gaussian radius w.
- Previous analyses favored $w \approx 1\,\text{fm}$.
  - This leads to a 3σ discrepancy in σ_{PbPb}.
- Fitting to the pPb and PbPb cross sections lowers w to 0.6 fm.
  - σ_{PbPb} discrepancy is reduced to 1σ.
  - Many other observables fit slightly worse.
- Smaller width is now compatible with our knowledge of the gluonic structure of the proton at low x.

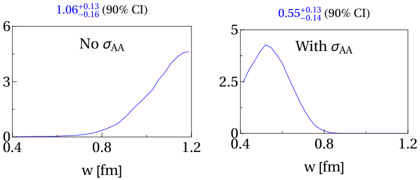

	σ_{PbPb}[b]	$\sigma_{p\text{Pb}}$[b]
with σ_{AA}	8.02 ± 0.19	2.20 ± 0.06
without σ_{AA}	8.95 ± 0.36	2.48 ± 0.10
ALICE/CMS	7.67 ± 0.24	2.06 ± 0.08

[GN, van der Schee, 2206.13522; ALICE, 2204.10148; CMS, 1509.03893; Caldwell, Kowalski, *Phys. Rev. C* **81** (2010) 025203]

Implication for $\rho(v_n\{2\}^2, \langle p_T \rangle)$

- Pearson correlation coefficient $\rho(v_n\{2\}^2, \langle p_T \rangle)$ between $v_n\{2\}^2$ and $\langle p_T \rangle$ is sensitive to the nucleon size.
- Postdiction without fitting to σ_{PbPb} and σ_{pPb} is qualitatively wrong:
  - $\rho(v_2\{2\}^2, \langle p_T \rangle)$ goes negative already at 30% centrality.
  - $\rho(v_3\{2\}^2, \langle p_T \rangle)$ has the wrong sign.
- Fitting to σ_{PbPb} and σ_{pPb} results in a much improved agreement.

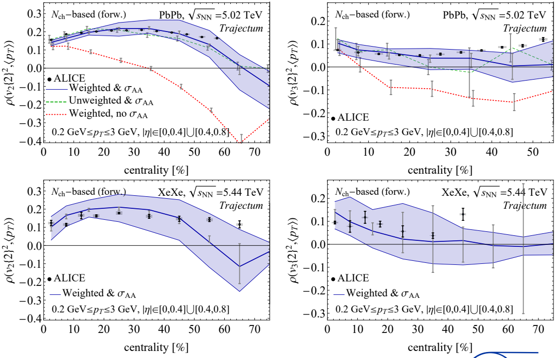

[GN, van der Schee, 2206.13522, Giacalone, Schenke, Shen, 2111.02908]

Nucleon width and $\rho(v_n\{2\}^2, \langle p_T \rangle)$

- Previous study shows that $\rho(v_n\{2\}^2, \langle p_T \rangle)$ depends strongly on the nucleon size w.

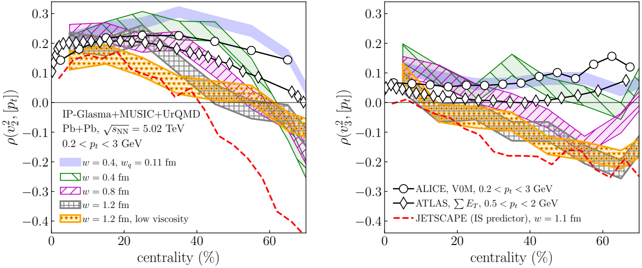

NLEFT densities

- We show the NLEFT densities for ^{16}O and ^{20}Ne.
- Densities are computed from configurations, requiring translation and rotation.
- This introduces biases, so we also show spherical configurations rotated in the same way to illustrate the size of this effect.

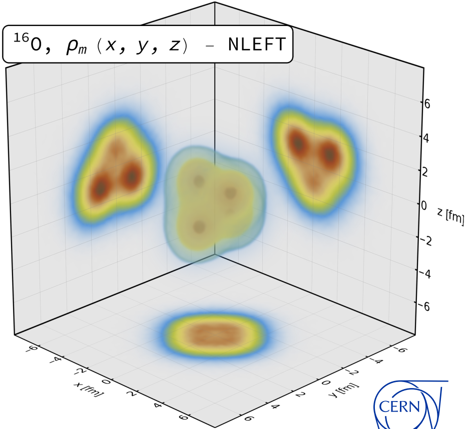

NLEFT densities

- We show the NLEFT densities for ^{16}O and ^{20}Ne.
- Densities are computed from configurations, requiring translation and rotation.
- This introduces biases, so we also show spherical configurations rotated in the same way to illustrate the size of this effect.

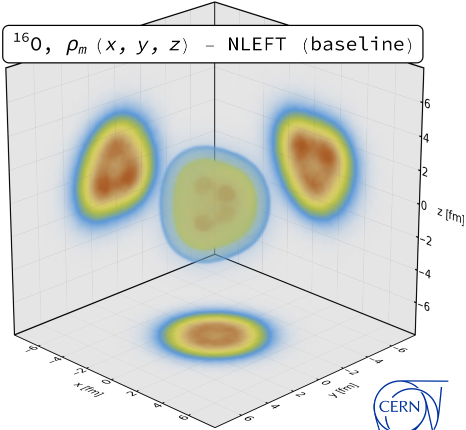

NLEFT densities

- We show the NLEFT densities for ^{16}O and ^{20}Ne.
- Densities are computed from configurations, requiring translation and rotation.
- This introduces biases, so we also show spherical configurations rotated in the same way to illustrate the size of this effect.

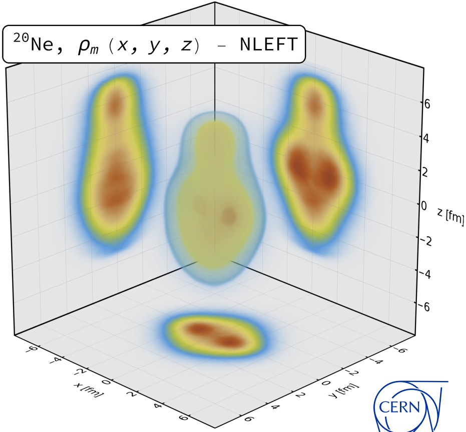

NLEFT densities

- We show the NLEFT densities for ^{16}O and ^{20}Ne.
- Densities are computed from configurations, requiring translation and rotation.
- This introduces biases, so we also show spherical configurations rotated in the same way to illustrate the size of this effect.

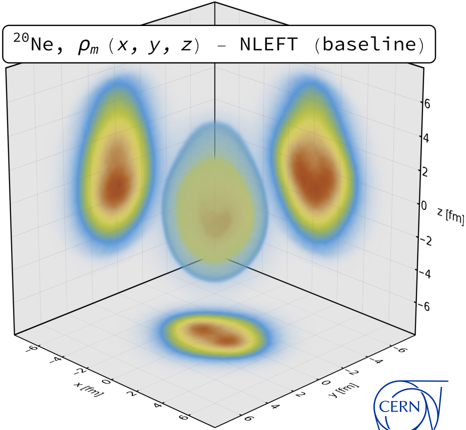

Other observables

- We show the NeNe/OO ratios for $\langle p_T \rangle$, $\delta p_T/\langle p_T \rangle$ and $v_3\{2\}$.
- Discrepancy in $\langle p_T \rangle$ between PGCM and NLEFT is due to the different nuclear charge radius.
- $\delta p_T/\langle p_T \rangle$ has interesting non-monotonic behavior for central collisions.

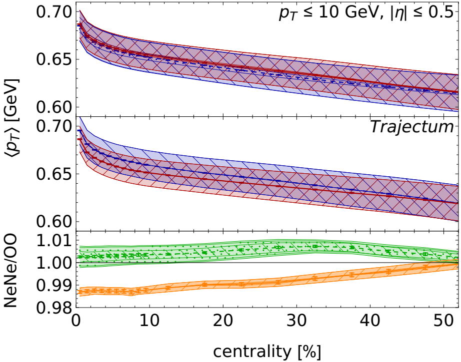

Other observables

- We show the NeNe/OO ratios for $\langle p_T \rangle$, $\delta p_T / \langle p_T \rangle$ and $v_3\{2\}$.
- Discrepancy in $\langle p_T \rangle$ between PGCM and NLEFT is due to the different nuclear charge radius.
- $\delta p_T / \langle p_T \rangle$ has interesting non-monotonic behavior for central collisions.

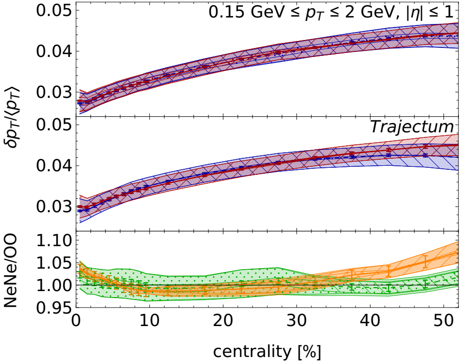

Other observables

- We show the NeNe/OO ratios for $\langle p_T\rangle$, $\delta p_T/\langle p_T\rangle$ and $v_3\{2\}$.
- Discrepancy in $\langle p_T\rangle$ between PGCM and NLEFT is due to the different nuclear charge radius.
- $\delta p_T/\langle p_T\rangle$ has interesting non-monotonic behavior for central collisions.

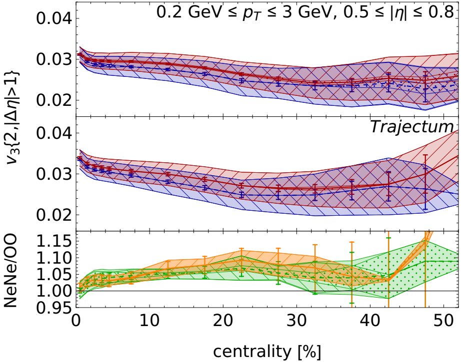

PGCM error ratios

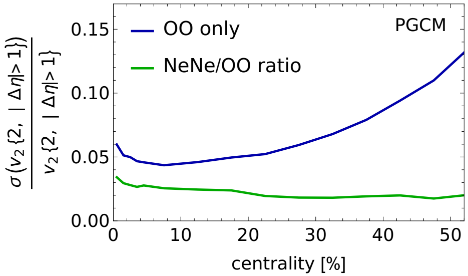

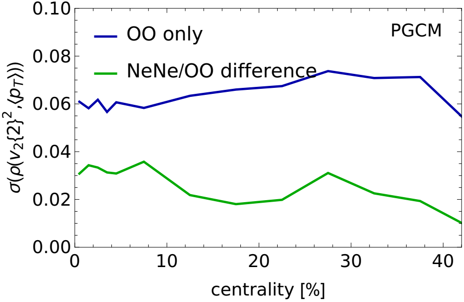

[Giacalone, Bally, GN, Shen et al., 2402.05995]

Why weights?

- Higher p_T, higher centralities are harder to model theoretically.
- Experimental correlation matrix is not available.
    - Figure shows 1σ and 2σ regions for $\rho \in \{0, 0.9, -0.9, 0.99\}$, with standard deviations the same.
    - Same difference between theory and experiment can be within 1σ or outside of 2σ depending on ρ.
    - Correlated observable classes can be over/underimportant for the Bayesian analysis.

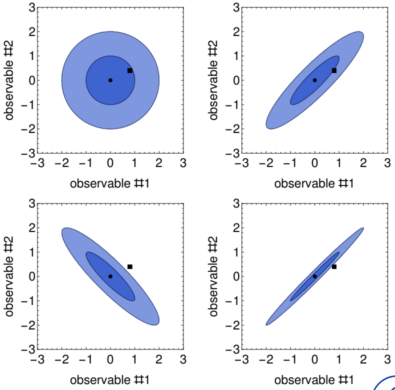

Definition of weights

- In the bayesian analysis, the probability of the data given the parameter point x is given by:

$$P(D|x) = \frac{1}{\sqrt{(2\pi)^m \det \Sigma}} \exp\left(-\frac{1}{2}(y - y_{\text{exp}})^T \Sigma^{-1} (y - y_{\text{exp}})\right),$$

with y the vector of observables computed from x, y_{exp} the vector of the corresponding experimental data, and Σ the combined theory/experiment covariance matrix.

- We define weights by replacing

$$P(D|x) = \frac{1}{\sqrt{(2\pi)^m \det \Sigma}} \exp\left(-\frac{1}{2}(y - y_{\text{exp}})^T \omega \Sigma^{-1} \omega (y - y_{\text{exp}})\right),$$

where ω is the diagonal matrix containing the weight for each observable.

Choice of weights

- We choose for weights ω:
  - 1/2 for every particle identified observable.
  - 1/2 for p_T-differential observables, and an additional $(2.5 - p_T[\text{GeV}])/1.5$ if $p_T > 1\,\text{GeV}$.
  - $(100 - c[\%])/50$ if the centrality class c is beyond 50%.
- Weighting only worsens the average discrepancy slightly.
- Distribution of discrepancies makes more sense.

	$\langle(y_{\text{theory}} - y_{\text{experiment}})/\sigma\rangle$				$\bar{\omega}$
	σ_{AA} & ω	ω	σ_{AA}	neither	
$dN_{\text{ch}}/d\eta$	0.55	0.60	1.23	1.22	1.00
$dN_{\pi^\pm,k^\pm,p^\pm}/dy$	0.76	0.70	0.60	0.57	0.48
$dE_T/d\eta$	1.59	1.51	0.82	0.77	0.48
$\langle p_T\rangle_{\text{ch},\pi^\pm,K^\pm,p^\pm}$	0.66	0.60	0.88	0.72	0.46
$\delta p_T/\langle p_T\rangle$	0.56	0.62	0.51	0.58	0.49
$v_n\{k\}$	0.58	0.51	0.54	0.49	1.00
$d^2N_{\pi^\pm}/dy\,dp_T$	1.19	1.07	0.86	0.92	0.20
$d^2N_{K^\pm}/dy\,dp_T$	1.41	1.27	0.79	0.73	0.20
$d^2N_{p^\pm}/dy\,dp_T$	1.35	1.21	0.73	0.67	0.25
$v_2^{\pi^\pm}(p_T)$	0.81	0.74	0.46	0.44	0.19
$v_2^{K^\pm}(p_T)$	0.92	0.89	0.55	0.55	0.19
$v_2^{p^\pm}(p_T)$	0.49	0.47	0.34	0.35	0.25
$v_3^{\pi^\pm}(p_T)$	0.65	0.57	0.69	0.57	0.24
average	0.89	0.83	0.69	0.66	
σ_{AA}	1.13	3.80	1.53	3.40	1.00

How much do weights change the posteriors?